

Mississippi State University

Scholars Junction

College of Arts and Sciences Publications and
Scholarship

College of Arts and Sciences

1997

Deposition of Conducting Polyaniline Patterns with the Scanning Electrochemical Microscope

David O. Wipf

Mississippi State University, dow1@msstate.edu

Junfeng Zhou

Mississippi State University

Follow this and additional works at: <https://scholarsjunction.msstate.edu/cas-publications>

Recommended Citation

Wipf, David O. and Zhou, Junfeng, "Deposition of Conducting Polyaniline Patterns with the Scanning Electrochemical Microscope" (1997). *College of Arts and Sciences Publications and Scholarship*. 33. <https://scholarsjunction.msstate.edu/cas-publications/33>

This Article is brought to you for free and open access by the College of Arts and Sciences at Scholars Junction. It has been accepted for inclusion in College of Arts and Sciences Publications and Scholarship by an authorized administrator of Scholars Junction. For more information, please contact scholcomm@msstate.libanswers.com.

Deposition of Conducting Polyaniline Patterns with the Scanning Electrochemical Microscope

Junfeng Zhou* and David O. Wipf**

Department of Chemistry, Box 9573, Mississippi State University, Mississippi State, MS 39762

(601) 325-3584, (601) 325-1618 [FAX], wipf@ra.msstate.edu

Abstract

Conducting polyaniline patterns were deposited on gold, platinum, and carbon surfaces with the use of the scanning electrochemical microscope (SECM). The patterns were deposited in the “micro-reagent” mode in which a local pH change caused by proton reduction at the SECM tip allowed deposition to occur at the substrate. The effect of tip and substrate potential, tip-substrate separation, and deposition time were studied in order to produce well-resolved patterns of the desired thickness. Lateral resolution of the deposited polymer was as low as 3 μm . Conductivity of the film was verified by SECM imaging.

"This document is the unedited Author's version of a Submitted Work that was subsequently accepted for publication in the Journal of the Electrochemical Society, copyright © 2002 ECS - The Electrochemical Society after peer review. To access the final edited and published work see

Citation Junfeng Zhou and David O. Wipf 1997 *J. Electrochem. Soc.* **144** 1202
<https://doi.org/10.1149/1.1837573>

*Electrochemical Society Student Member

**Electrochemical Society Active Member

Submitted to *J. Electrochem Soc.*, August 12, 1996

Revised version submitted December, 2 1996

Recent interest in conducting polymers has been on the ability to prepare microscopic features as a step in the construction of organic semiconducting devices such as transistors, logic gates, and light-emitting diodes.¹⁻⁵ In many cases these conducting or semiconducting polymer devices are formed on a substrate in a bulk fashion by coating the entire part with the desired polymer film and then using traditional microlithographic techniques to form the desired structure. An alternate method is to draw directly the desired polymer structure on the substrate. In this paper a method is described for direct patterning of microscopic conducting polyaniline features on conductive substrates by use of the scanning electrochemical microscope (SECM).

The SECM is a scanned-probe microscope designed for making images of surfaces immersed in an electrolyte solution. A number of recent reviews have described operation of the SECM.⁶⁻⁸ In addition to its use as an imaging device, the SECM has also been extensively used as a microfabrication tool. There are two quite different methods that have been put into effect for SECM microfabrication. The earliest method is the "direct" mode of operation.⁹⁻¹³ In the direct mode, the tip serves as a microscopic auxiliary electrode to an anodic or cathodic conducting substrate. Because of the tip's small size and close spacing, current at the substrate is confined to a small area. Both metal etching^{9,10} and deposition¹² (using the tip as a sacrificial source of metal) as well as polymer deposition have been reported using this mode.^{11,14,15}

Polyaniline deposition by the direct mode was first reported by Bard and coworkers.¹¹ In this report, deposition was accomplished by coating the surface with a thin Nafion film containing the aniline monomer. Using a sharp, STM-type tip, a thin (2 μm) polyaniline pattern was made on the anodic substrate. The Nafion film served to limit the spread of current away from the tip by restricting ionic movement and thus allowed for finer resolution in the deposited film. In another application of the direct mode for polymer deposition, Kranz and coworkers have been able to deposit lines of polythiophene from free solution.^{14,15}

The other mode used for SECM microfabrication is a "micro-reagent" mode. Here the surface is modified by using the SECM tip to electrogenerate reagents and a variety of applications have been

described. Shohat and Mandler deposited NiOOH patterns by causing a local pH increase at the SECM tip.¹⁶ Ratcliff and coworkers have recently demonstrated localized dissolution of a carbon oxide layer by the generation of OH⁻ ions.¹⁷ Metals¹⁸ and semiconductors^{19,20} can be etched by electrogeneration of oxidants. Sugimura and coworkers made fluorescent micropatterns in an ionomeric film by locally decreasing the concentration of a fluorescent quencher.²¹ An advantage of the micro-reagent mode over the direct mode is that the substrate need not *necessarily* be electronically conducting. Also, since the modification process at the substrate is chemical, there are a larger number of possible types of modification reactions. To our knowledge, no reports of polymer deposition using the micro-reagent mode have been reported.

In addition to deposition of conducting polymers, SECM has also been used to image and characterize them. The ingress and egress of ions during the oxidation and reduction of conducting polymers has been observed with the SECM.²²⁻²⁷ Detection of the conductivity change of polymers during oxidation and reduction has also been reported.^{24,28-30}

In this report, we exploit the pH dependence of the oxidation potential of the aniline monomer to prepare microscopic patterns of conducting polyaniline by use of the SECM micro-reagent mode. Deposition of the polymer is possible by generating a local increase in pH at the SECM tip by proton or water reduction (Figure 1). Polymer patterns are generated in various thicknesses and with widths as small as 3 μm . Conductivity of the polyaniline patterns is verified by SECM imaging and by a direct electrical measurement.

Experimental

Reagents. Aniline (98%, Aldrich), hexaammineruthenium(III) chloride (Strem Chemicals), and all other chemicals were used as received. All solutions were prepared with 18 M Ω distilled-deionized water.

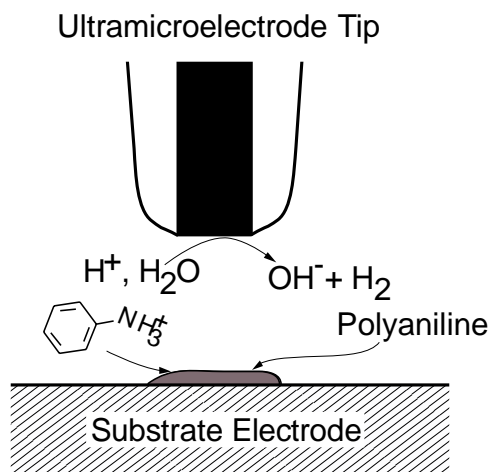


Figure 1. Illustration of the SECM polyaniline deposition process.

Electrodes. The three tip electrodes used here, the 100, 10, and 2 μm diameter Pt and the 8 μm diameter carbon-fiber electrode, were prepared according to previously published methods for construction of ultramicroelectrodes and SECM tips.^{31,32} All the ultramicroelectrodes had a disk-shaped geometry. Three different electrodes were used as substrates for the deposition of polyaniline: a glassy-carbon (GC) electrode (BAS, West Lafayette, IN), a home-made platinum disk electrode, and an evaporated gold film electrode. The evaporated gold film electrode consisted of a 5 nm Cr adhesion layer and a 100 nm layer of Au deposited on a glass microscope slide. All the above electrodes were polished before each experiment with a slurry of 0.05 μm alumina on cloth except for the Au film electrode, which was used as prepared.

All experiments used a Ag/AgCl (3 M NaCl) reference electrode and all potentials are referred to this. The auxiliary electrode was a Pt wire.

Instrumentation. All electrochemical experiments, except for SECM experiments, were made with use of the BAS 100B/W electrochemical workstation (BAS, West Lafayette, IN). The SECM equipment has been described previously.³³ During the SECM experiments, simultaneous potential control of both the tip and substrate was accomplished with the use of a bipotentiostat (EI-400, Ensmann Instrumentation, Bloomington IN). For the polymer deposition and imaging experiments the electrochemical cell was constructed such that the substrate electrode was positioned at the cell bottom, facing up, and the tip was positioned normal to and above the electrode surface.

Experimental Procedure. In general, the procedure for polyaniline deposition was as follows: The aniline solution was introduced into the SECM cell and the substrate electrode potential was adjusted to a value more positive than 0 V vs Ag/AgCl such that no faradaic current was observed. The tip was brought to the surface in one of two ways. One method is to lower the tip slowly to the surface until the tip and substrate touched and caused an electrical short circuit. A large current flowing at both the tip and substrate indicated this condition. This method sometimes damaged the tip or substrate so a second method was used. In the second method a negative potential at the tip caused proton reduction. The tip was then lowered until a characteristic tip current decrease due to negative feedback was observed. At this point the tip was “at the surface”. Using either of the two methods, the tip was then brought back to the desired experimental distance from the surface. The tip was then usually moved laterally away from the initial point of contact to avoid any disturbance in the experimental results due to the close tip-substrate distance during the approach. Once the tip was positioned appropriately, the experiment commenced by applying the appropriate potentials at the tip and substrate. More experimental details are given in the Results and Discussion section.

Results and Discussion

Effect of Proton Concentration on the Aniline Oxidation. A number of reports have been published that comment on the joint effects of proton concentration and electrolyte anion identity on the electrochemical synthesis of polyaniline.³⁴⁻³⁶ Shown in Figure 2 are the initial voltammograms of a solution of 100 mM aniline in 2, 0.1, 0.01 M H₂SO₄ at an 8 μm diameter carbon-fiber microelectrode. As is quite clearly seen in the Figure, the aniline oxidation potential shifts to more positive values as the proton concentration increases. Additional voltammetric cycles in the 2 and 0.1 M H₂SO₄/aniline solution (not shown) do show the characteristic oxidation and reduction peaks for polyaniline.^{35,37} In addition, these peaks increase in height with cycling, indicating deposition of a conducting film. In contrast, subsequent cycles in 0.01 M H₂SO₄/aniline solution show no evidence of growth of a conducting polymer film. However, a thin poorly conducting film is formed in this solution. If an electrode cycled in the 0.01 M

H_2SO_4 /aniline solution is transferred to a blank 2 M H_2SO_4 solution and then cycled, a set of small oxidation/reduction waves are observed. These are similar in position to those waves of the polyaniline film grown in the more acidic solutions. However, these waves disappeared with subsequent cycling and it appears that this thin film is unstable. Thus it appears that a poorly conducting film grown in 0.01 M H_2SO_4 solution can be made conductive by exposure to a higher acidity solution.

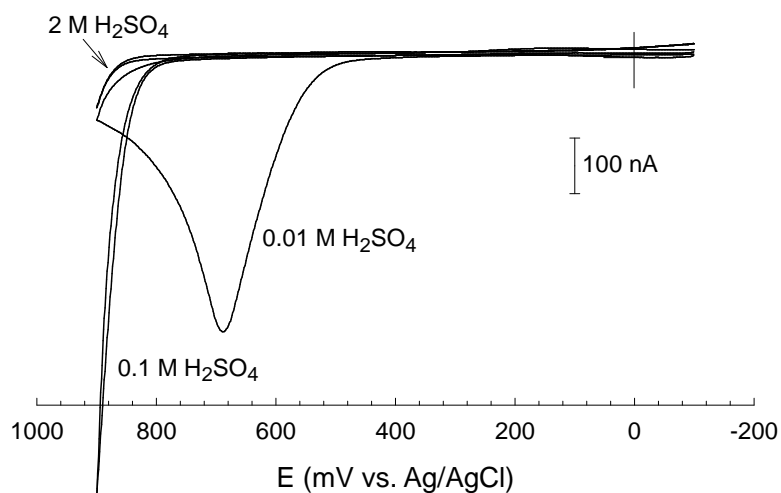


Figure 2. Cyclic voltammograms of 100 mM aniline in 2, 0.1, and 0.01 M H_2SO_4 solution at an 8 μm diameter carbon-fiber microelectrode. The scan rate is 100 mV/s and the cross indicates the zero current and potential point.

Polyaniline films can also be deposited at a constant potential.^{38,39} Since the SECM deposition process uses a constant potential, a few experiments were performed to verify the literature reports. Experiments in which an electrode was polarized at 700, 800, and 900 mV in a 2 M H_2SO_4 solution containing 100 mM aniline all subsequently gave an electrode film similar to that formed by potential cycling. After growing the film at a constant potential, voltammograms of the film-coated electrode gave oxidation-reduction waves in 2 M H_2SO_4 similar to those of polymer-coated electrodes grown by the potential cycling method. Films grown at less positive potentials gave smaller currents upon cycling and thus appeared to be thinner than the films grown at more positive potentials. No film growth was observed when the electrode was poised at 300 mV in the aniline/ H_2SO_4 solutions.

SECM Patterning of Polyaniline Features. As illustrated in Figure 1, the SECM can be used to locally reduce the proton concentration by reduction of protons and/or water at the SECM tip. Therefore, a localized deposition of polyaniline features can be made by taking advantage of the proton concentration sensitivity of aniline oxidation. With the tip positioned close to an electrode surface only a small region of the surface will experience a local proton concentration decrease. By starting with a concentrated acid solution and biasing the substrate just negative of the point at which aniline would be oxidized in that solution, bulk polymerization over the entire surface is prevented. However, at the tip position the proton concentration is decreased, the potential for aniline oxidation is thus more negative, and local polymer deposition occurs. In this case, the polymer modification is by the micro-reagent mode.

Of interest is the ability to control the polymer feature size (width) and thickness of the film. In addition, control of the polymer's conductivity would be useful. The following experimental variables were examined for their effect on the deposited polyaniline feature size and thickness: tip dimension, tip potential (or current), substrate potential, deposition time, and tip-substrate separation.

The effect of tip size is somewhat expected. For the microdisk electrodes employed here, the minimum size of any feature is that of the disk electrode itself. The simplest feature made is a 'dot' feature constructed by positioning the tip at a single position and allowing the local SECM deposition to take place. Figure 3 shows dot features made using 100 and 2 μm diameter platinum tip electrodes.

Two very important variables in the polyaniline deposition process are the tip and substrate potentials. It is critically important to control the substrate potential sufficiently positive so that aniline oxidation will occur in the higher pH region around the tip but not so positive that polymerization will occur at the lower pH over the remainder of the electrode surface. For most of the experiments reported here a substrate potential of 600 mV vs. Ag/AgCl was used in solutions of 2 M H_2SO_4 . In some initial experiments, a substrate potential of 700 mV was used. This potential gave excellent deposition results but was found to lead to a thin but visible polymer layer on the Pt substrate electrode surface after about an hour of experimentation. In contrast, a substrate potential of 500 mV gave very poor or no polymer deposits.⁴⁰ The dots in Figure 3 were deposited at a substrate potential of 600 mV.

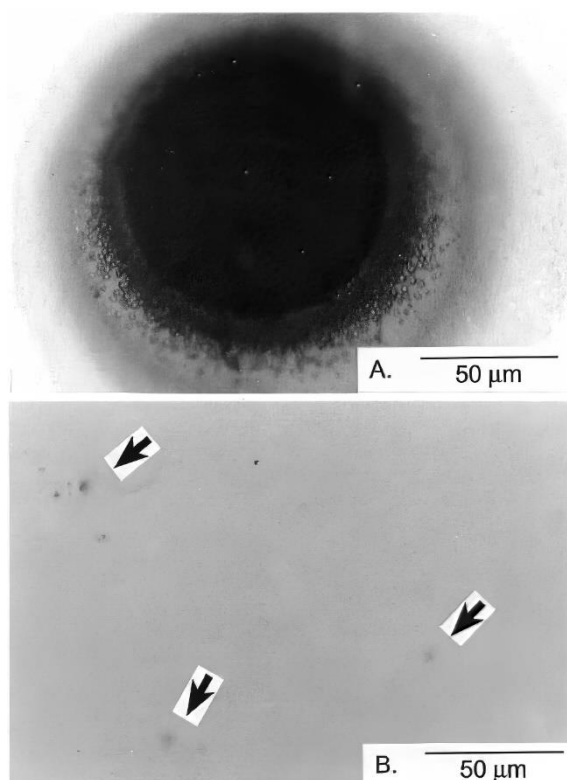


Figure 3. Light microscope images of polyaniline dots deposited on a Pt substrate biased at 600 mV. The deposition solution was 100 mM aniline in 2 M H₂SO₄. A). Deposition conditions: 100 μm diameter Pt tip, tip potential is -1200 mV, deposition time is 120 s, and tip-substrate separation is 30 μm. B). Deposition conditions: 2 μm diameter Pt tip, tip potential is -1500 mV, deposition time is 120 s, and tip-substrate separation is 0.5 μm.

The potential at the tip must be negative enough to give a large local decrease in proton concentration. In general, potentials near the limiting current for the proton reduction were used.²⁷ At the 100 μm diameter Pt tip a -1200 mV bias gave a cathodic current of about 1 mA (12 A/cm²). This is sufficient to deposit polyaniline at a substrate biased at 600 mV. Potentials slightly more negative or positive of -1200 mV gave polyaniline deposits that appeared slightly darker or lighter in color, respectively, suggesting a thicker or thinner deposit. No deposit is observed with a tip potential of -800 mV and a substrate potential of 600 mV.

At smaller tips the potential required to get good polyaniline deposits shifts negative. At a 10 μm diameter tip, a better deposition potential is -1400 mV where a current of about 100 μA (125 A/cm²) flows. At a 2 μm diameter tip, tip potentials more negative than -1500 mV are required.

More complicated features than dots can be generated by scanning the tip laterally across the substrate surface to draw a polymer pattern. In this case, the tip scan speed and tip-substrate separation must be considered. A pattern deposited on a glassy-carbon electrode (Figure 4) shows the effect of tip scan speed. The top and bottom edges of the square pattern are deposited with a 10 μm Pt tip at a distance of about 2 μm and at a scan speed of 1.0 $\mu\text{m}/\text{s}$, top, and 0.1 $\mu\text{m}/\text{s}$, bottom. The top edge's width and thickness are more uniform than the bottom edge. The ragged bottom edge is thought to be a consequence of the slow tip movement allowing the film to grow to completely fill the gap between the tip and substrate and, perhaps, be subject to mechanical damage from the tip movement. In addition, polymer film is spreading away from the main deposit, degrading resolution. So in this case, a more rapid tip movement is preferred.

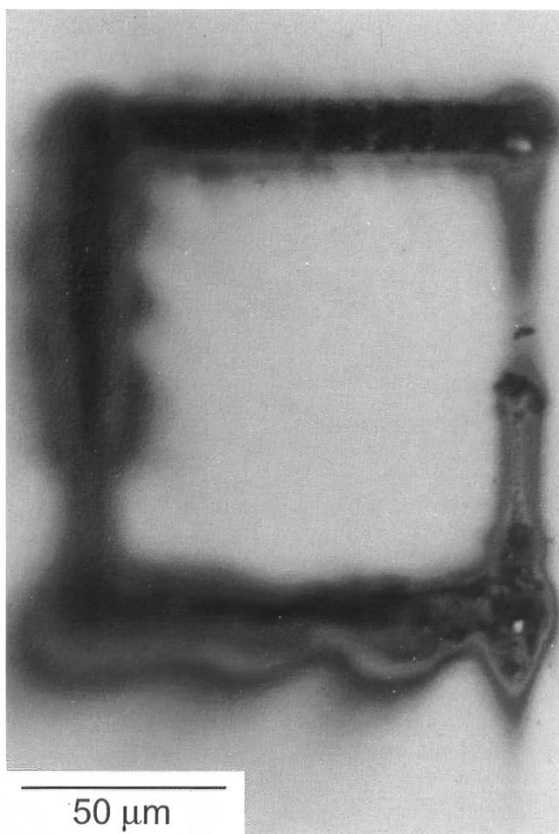


Figure 4. Light microscope image of a polyaniline pattern deposited on a glassy-carbon substrate using a 10 μm Pt tip electrode. Deposition conditions: substrate potential is 600 mV, tip potential is -1300 mV, tip-substrate separation is about 2 μm , and tip scan speed ranged from 0.1 (bottom line) to 1.0 (top line) $\mu\text{m}/\text{s}$.

Tip-substrate separation also greatly influences the deposition process. Figure 5 is an optical micrograph of a study of the effect of tip-substrate separation on the deposited film. In this case, the deposit was made on a Au electrode with a 10 μm Pt tip set at a potential of -1400 mV vs Ag/AgCl. The tip scanning speed was 0.5 $\mu\text{m}/\text{s}$. A consecutive series of 40 μm long lines were drawn at separations of 1 to 5 μm . At the 1 and 2 μm separations there is a dark greenish-black core exactly 10 μm wide with a halo of blue, green, and yellow film areas extending away from the core. The core has a granular appearance that is quite distinct from the surrounding area. In addition, the core area of film formed at a 1 μm separation appeared under the microscope to have a flat top. This suggests that this film and the 2 μm separation film grew to the thickness of the gap during the time of the scan. In support of this, it was noted that large tip and substrate current fluctuations occurred during the 1 and 2 μm separation depositions. The tip and substrate current fluctuations were greater than 3 mA, were correlated in time and magnitude, and were opposite in sign. It is likely that these current fluctuations were due to the polyaniline film “shorting out” the tip and substrate. The shorting current observed allows a rough estimate of the conductivity of the polyaniline film by use of the following equation.

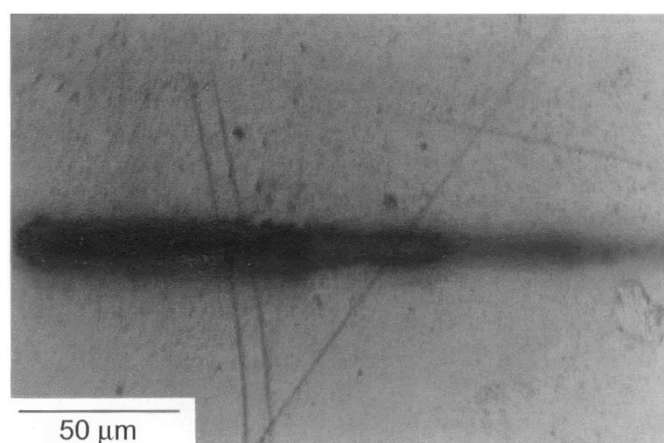


Figure 5. The effect of tip-substrate separation is shown in this light microscope image of a polyaniline pattern deposited on a Au substrate using a 10 μm Pt tip electrode. From left to right successive 40 μm long lines were drawn at separations from 1 to 5 μm . Other deposition conditions: substrate potential is 600 mV, tip potential is -1400 mV, and tip scan speed is 0.5 $\mu\text{m}/\text{s}$.

$$\kappa = \frac{L}{RA}$$

where κ is the conductivity in S cm^{-1} , R is the resistance in ohms, L is the length of the conductor, and A is the area of contact. For a 2.0 V potential difference (0.6 V substrate and -1.4 V tip) a current of greater than 3 mA was observed at a region 1 μm thick and an area of about $8 \times 10^{-7} \text{ cm}^2$ ($r = 5 \mu\text{m}$). Thus, the estimated conductivity is about 0.18 S cm^{-1} . This is at the low end of the range of conductivity reported for polyaniline^{34,36} but it is likely to be a very low estimate, since the area of contact is unlikely to be the entire electrode area but a smaller polyaniline strand.

At greater tip-substrate separations, the film loses the core area, becomes lighter in color, and appears to become progressively thinner as the separation increases. The film at 3 μm separation is bluish-green color, at 4 μm it is green, and at 5 μm it is yellow-green in color.

The effect of tip-substrate separation, tip potential, and deposition time are strongly coupled. Close separations allow use of shorter deposition times or lower tip potentials. Alternately, the thickness of the film can be controlled by tip-substrate separation, deposition time, or tip potential. There does not appear to be a unique set of conditions required to produce a film pattern on a surface. It is likely that the film properties do change with the above variables. For example, it is not yet clear if there is a difference other than thickness in the film formed at close separations with the core feature and the film formed at larger separations without the core.

A photograph of a more complicated pattern is shown in Figure 6a. This was drawn on an Au substrate biased at 600 mV vs. Ag/AgCl. The 10 μm Pt tip was set at -1400 mV and was scanned at 0.5 $\mu\text{m/s}$ at a separation of about 1 μm from the surface. Figure 6b shows a higher magnification photograph of the pattern in Figure 6a. The core feature is evident and the total line-width is around 18 μm . A higher lateral resolution is obtained for the 50 μm long line above the U in Figure 6a. This was drawn at a separation of about 2 μm .

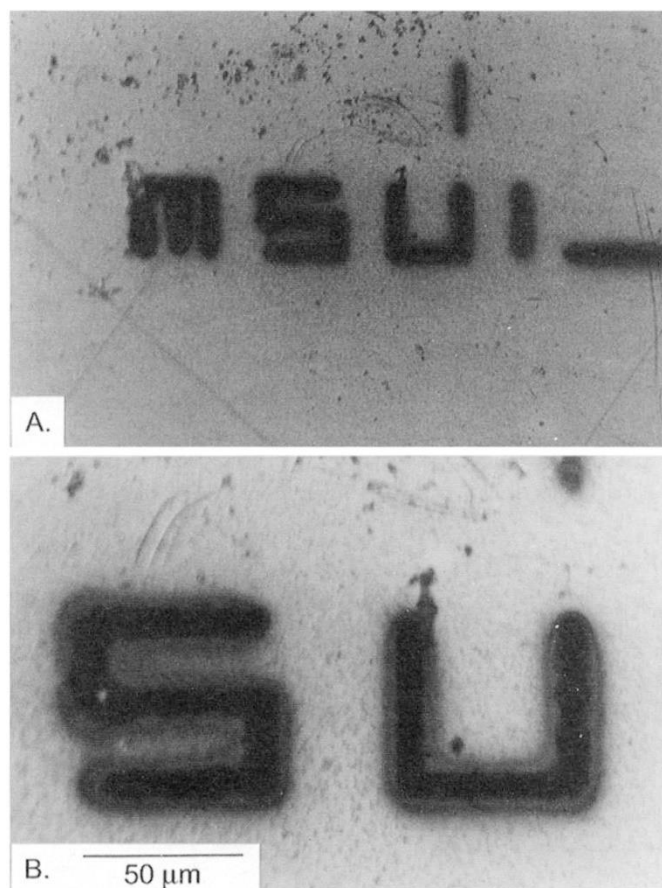


Figure 6. A light microscope image of a polyaniline pattern deposited on a Au substrate using a 10 μm Pt tip electrode. Figure B. is a magnification of part of figure A. Deposition conditions: substrate potential is 600 mV, tip potential is -1400 mV, tip-substrate separation is about 1 μm , and the tip scan speed is 0.5 $\mu\text{m/s}$.

Higher resolution pattern deposition can only be accomplished with use of a smaller tip electrode. Although dot-type features were made with a smaller (2 μm dia.) Pt tip (Figure 3b), making lines or more complicated features proved elusive. There were a number of problems that appeared to contribute to the difficulty. One is the fragility of the tip. Several 2 μm tips failed during deposition due to a large current flow during a tip-substrate or tip-polyaniline-substrate short circuit. This was apparently due to melting and internal disconnection of the micro-Pt wire making up the electrode. Attachment of a 100 k Ω resistor in series with the tip electrode limits the current flow possible during short-circuit events and prevents damage. The resistor will also cause a small Ohmic drop during deposition but this can be compensated by

increasing the tip potential. A second possible problem may be a difficulty in achieving the decrease in proton concentration required for successful deposition. It is postulated that at the smaller tips the protons diffuse back more quickly to the electrode location thus requiring a higher current density to achieve deposition. This is supported by the observation that the 10 μm diameter tip requires about a 10 fold higher current density than the 100 μm tip to achieve good deposition. Another possible problem is blocking by H_2 bubbles formed during the proton reduction. H_2 bubbles may also stir the solution and prevent the required pH increase. It may be possible to increase the pH under the tip without forming H_2 bubbles. For example, by quinone reduction at the tip. Despite these problems, it is not yet clear that forming higher resolution features is impossible. The fact that dot features are formed is a hopeful sign that the deposition of more complicated features at high resolution is possible.

SECM Imaging of Polyaniline Features. SECM imaging of the deposited polyaniline patterns also verify their conductivity. Figure 7 is an SECM image made of a pattern deposited on a Pt substrate. This image was made using a 10 μm Pt disk tip electrode at a scan rate of 10 $\mu\text{m/s}$. The mediator was a 2 mM solution of $\text{Ru}(\text{NH}_3)_6^{3+}$ ion in 2 M H_2SO_4 . During imaging, the tip was biased at -100 mV and the substrate was biased at 600 mV. At these potentials the polyaniline would be expected to be in a conductive state. The image shows a clear pattern of lines showing up at higher currents. In this case, since the polyaniline features protrude from the surface, the implication is that they must be conductive to show a larger current than the remainder of the image. If this image is compared to the optical micrograph in Figure 8, a good correspondence is seen between the higher current features in the SECM image and the polyaniline pattern in the photograph. Notice that the film was somewhat damaged during or after scanning. The larger current in the upper left corner of the SECM image is probably due to an electrical short circuit between the tip and the polyaniline film during scanning. This correlates with damage in the same region of the optical micrograph. It should be noted that -100 mV tip bias used during SECM imaging is not sufficiently negative to give a limiting current for the reduction of the $\text{Ru}(\text{NH}_3)_6^{3+}$ ion, so the observed imaging current in Figure 7 is less than one might expect. The lower potential was chosen to avoid interference from proton reduction and does not alter the conclusion that the polyaniline pattern is conductive.

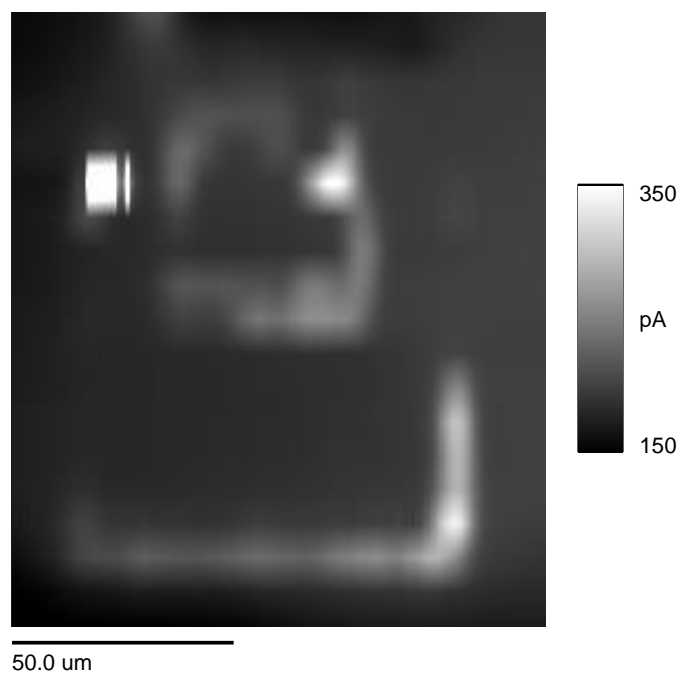


Figure 7. SECM image of a polyaniline pattern deposited on a Pt substrate. Scanning parameters: mediator, 2.0 mM $\text{Ru}(\text{NH}_3)_6^{3+}$ in 2 M H_2SO_4 ; tip, Pt disk at -100 mV; substrate potential, 600 mV; tip-scan speed, 10 $\mu\text{m/s}$.

SECM images made of the polyaniline film when the substrate was biased at 750 and 900 mV had much larger currents, were “noisy”, and did not give recognizable images of the pattern.⁴⁰ After these scans, subsequent images made at lower potentials did not show a conductive pattern or in fact any recognizable feature. This behavior is attributed to a degradation reaction at the higher potentials leading to a loss in film conductivity and the production of *p*-benzoquinone.⁴¹ The large currents and “noise” observed at the higher potential scans were likely due to the reduction of the *p*-benzoquinone at the SECM tip.



Figure 8. Optical micrograph of the polyaniline pattern imaged in Figure 7. Deposition conditions: 10 μm diameter Pt tip at -1200 mV, Pt substrate at 600 mV, tip-substrate separation is about 2 μm , and the tip scan speed is 1.0 $\mu\text{m/s}$.

Conclusions

Microscopic patterns of conducting polyaniline can be prepared on platinum, carbon, and gold electrode by use of the SECM. The resolution of the patterns is demonstrated on the micrometer scale and is governed primarily by the size of the SECM tip. The polymer deposition is mainly driven by a micro-reagent mode, not previously described, in which a local pH increase at the SECM tip provides a condition necessary to polymerize aniline on the substrate. Pattern deposition does occur over a wide range of experimental variables. The most critical variable appears to be the substrate potential. The tip potential, tip scan speed, and tip-substrate separation are tightly linked and it appears that there are no unique values of these variables required for polyaniline deposition.

SECM imaging is used to confirm that the deposited film is in a conductive state at the potentials and solutions used in this paper. In addition, the magnitude of the short-circuit current that flowed through the film allows an estimate of the polyaniline conductivity of at least 0.18 S cm^{-1} .

Acknowledgments

Acknowledgment is made to the National Science Foundation (CHE-94144101) for providing financial support for this research. The authors thank Dr. Yeon-Taik Kim for the donation of the evaporated gold film electrodes.

References

1. J. H. Burroughes, D. D. C. Bradley, A. R. Brown, R. N. Marks, K. Mackay, R. H. Friend, P. L. Burns and A. B. Holmes, *Nature*, **347**, 539 (1990).
2. G. Gustafsson, Y. Gao, G. M. Treacy, F. Klavetter, N. Colaneri and A. J. Heeger, *Nature*, **357**, 477 (1992).
3. F. Garnier, R. Hajlaoui, A. Yassar and P. Srivastava, *Science*, **265**, 1684 (1994).
4. A. J. Heeger, D. J. Heeger, J. Langan and Y. Yang, *Science*, **270**, 1642 (1995).
5. G. P. Kittlesen, H. S. White and M. S. Wrighton, *J. Am. Chem. Soc.*, **106**, 7389 (1984).
6. A. J. Bard, F.-R. Fan and M. Mirkin, in *Physical Electrochemistry: Principles, Methods, and Applications*, I. Rubenstein, Editor, p. 209, Marcel Dekker, New York, (1995).
7. A. J. Bard, F.-R. Fan and M. V. Mirkin, in *Electroanalytical Chemistry*, A. J. Bard, Editor, Vol. 18, p. 244, Marcel Dekker, New York, (1994).
8. M. Arca, A. J. Bard, B. R. Horrocks, T. C. Richards and D. A. Treichel, *Analyst*, **119**, 719 (1994).
9. O. E. Hüsser, D. H. Craston and A. J. Bard, *J. Electrochem. Soc.*, **136**, 3222 (1989).
10. O. E. Hüsser, D. H. Craston and A. J. Bard, *J. Vac. Sci. Technol.*, **6**, 1873 (1988).
11. Y.-M. Wu, F.-R. F. Fan and A. J. Bard, *J. Electrochem. Soc.*, **136**, 885 (1989).
12. S. Meltzer and D. Mandler, *J. Electrochem. Soc.*, **142**, L82 (1995).
13. D. H. Craston, C. W. Lin and A. J. Bard, *J. Electrochem. Soc.*, **135**, 785 (1988).
14. C. Kranz, M. Ludwig, H. E. Gaub and W. Schuhmann, *Adv. Mater.*, **7**, 568 (1995).
15. C. Kranz, M. Ludwig, H. E. Gaub and W. Schuhmann, *Adv. Mater.*, **7**, 38 (1995).
16. I. Shohat and D. Mandler, *J. Electrochem. Soc.*, **141**, 995 (1994).
17. B. B. Ratcliff, J. W. Klancke, M. D. Koppang and R. C. Engstrom, *Anal. Chem.*, **68**, 2010 (1996).

18. D. Mandler and A. J. Bard, *J. Electrochem. Soc.*, **136**, 3143 (1989).
19. D. Mandler and A. J. Bard, *Langmuir*, **6**, 1489 (1990).
20. D. Mandler and A. J. Bard, *J. Electrochem. Soc.*, **137**, 2468 (1990).
21. H. Sugimura, T. Uchida, N. Shimo, N. Kitamura and H. Masuhara, *Ultramicroscopy*, **42**, 468 (1992).
22. M. Arca, M. V. Mirkin and A. J. Bard, *J Phys Chem*, **99**, 5040 (1995).
23. J. Kwak and F. C. Anson, *Anal. Chem.*, **64**, 250 (1992).
24. C. M. Lee and A. J. Bard, *Analytical Chemistry*, **62**, 1906 (1990).
25. C. Lee and F. C. Anson, *Anal. Chem.*, **64**, 528 (1992).
26. M. H. T. Frank and G. Denuault, *J Electroanal Chem*, **354**, 331 (1993).
27. M. H. T. Frank and G. Denuault, *J Electroanal Chem*, **379**, 399 (1994).
28. J. Y. Kwak, C. M. Lee and A. J. Bard, *J. Electrochem. Soc.*, **137**, 1481 (1990).
29. I. C. Jeon and F. C. Anson, *Anal. Chem.*, **64**, 2021 (1992).
30. F. R. F. Fan, M. V. Mirkin and A. J. Bard, *J Phys Chem*, **98**, 1475 (1994).
31. R. M. Wightman and D. O. Wipf, in *Electroanalytical Chemistry*, A. J. Bard, Editor, Vol. 15, p. 267, Marcel Dekker, New York, (1989).
32. D. O. Wipf and A. J. Bard, *J. Electrochem. Soc.*, **138**, 469 (1991).
33. D. O. Wipf, *Coll. Surf. A*, **93**, 251 (1994).
34. A. G. MacDiarmid and A. J. Epstein, *Faraday Discuss. Chem. Soc.*, **88**, 317 (1989).
35. L. Duic and Z. Mandic, *J. Electroanal. Chem.*, **335**, 207 (1992).
36. R. Saraswathi, S. Kuwabata and H. Yoneyama, *J. Electroanal. Chem.*, **335**, 223 (1992).
37. G. Inzelt, in *Electroanalytical Chemistry*, A. J. Bard, Editor, Vol. 18, p. 89, Marcel Dekker, New York, (1994).
38. W.-S. Huang, B. D. Humphrey and A. G. MacDiarmid, *J. Chem. Soc., Faraday Trans. 1*, **82**, 2385 (1986).
39. B. C. Sherman, W. B. Euler and R. R. Forcé, *J. Chem. Ed.*, **71**, A94 (1994).
40. J. Zhou, MS Thesis, Mississippi State University, Mississippi State, MS, (1996).
41. T. Kobayashi, H. Yoneyama and H. Tamura, *J. Electroanal. Chem.*, **177**, 293 (1984).